

Measurement of the effect of moderate dissipation on macroscopic quantum tunneling

Andrew N. Cleland, John M. Martinis,* and John Clarke

*Department of Physics, University of California, Berkeley, California 94720
and Materials and Chemical Sciences Division, Lawrence Berkeley Laboratory,
Berkeley, California 94720*

(Received 9 November 1987)

The escape rate $\Gamma(T)$ from the zero voltage state has been measured for a current-biased Josephson tunnel junction shunted with a normal metal resistor. Values of $\Gamma(T)$ measured at the lowest temperature of the experiment, 18 mK, and extrapolated to $T=0$ are in excellent agreement with the predictions for macroscopic quantum tunneling that include a reduction by a factor of about 300 for the effect of dissipation. Above the crossover temperature, the enhancement of $\Gamma(T)$ over the rate for thermal activation is in good agreement with predicted quantum corrections.

The current-biased Josephson junction and the flux-biased superconducting quantum interference device (SQUID) are ideal for measuring the effects of dissipation and temperature on macroscopic quantum tunneling (MQT).¹ Theory predicts that at $T=0$, dissipation exponentially reduces the tunneling rate Γ from the zero voltage state,^{1,2} that for $0 < T < T_{cr}$ (the crossover temperature) the tunneling rate is enhanced³⁻⁸ over that at $T=0$, and that for $T > T_{cr}$ quantum effects increase^{3,9,10} the escape rate over Kramer's result for thermal activation.¹¹ After the early experiments of Ouboter and co-workers,¹² Voss and Webb,¹³ and Jackel *et al.*,¹⁴ several other measurements of MQT have been made; a complete listing appears in Ref. 15. In particular, measurements on current-biased junctions with low dissipation¹⁵ showed that the MQT rate became independent of temperature at low temperatures with a value in good agreement with the predictions for $T=0$. However, the predicted effects of dissipation and temperature on the escape rate are less well confirmed. Washburn, Webb, Voss, and Faris¹⁶ varied the dissipation by fabricating a series of junctions with different shunt capacitances. They were able to fit their data by the predictions at $T=0$ for the lower capacitances but not for the higher. Furthermore, to calculate the dissipation the authors used the resistance R_N of the junction measured at voltages above $2\Delta/e$ (Δ is the energy gap of the Nb electrodes) although "it is not obvious that R_N measures the damping that appears in the theory." The same authors also found that $\ln[\Gamma(T)/\Gamma(0)] = (T/T_Q)^2$ for $T < T_{cr}$ as predicted, but that the value of T_Q was approximately a factor of $\sqrt{2}$ smaller than the predicted value. Schwartz, Sen, Archie, and Lukens¹⁷ measured the escape rate on a SQUID in which the junction, shunted with a metal film, was in the overdamped limit, measuring the relevant parameters in the classical regime. Their data exhibited both the T^2 dependence of $\ln\Gamma(T)$ and the predicted value of T_Q , but there was a major discrepancy between the measured and predicted values of the prefactor of the tunneling exponent, leading the authors¹⁸ to question the applicability of the theory.

However, Grabert and Weiss¹⁸ commented that the discrepancy could be resolved by choosing a slightly different value of critical current. Subsequently, Lukens and co-workers¹⁹ used the theory of Zaiken and Panyukov²⁰ to recompute the critical current and found reasonable agreement between the measured and predicted rates of macroscopic quantum tunneling for $T \lesssim T_{cr}$. On the other hand, for $T \gtrsim T_{cr}$ the uncertainties in the data were comparable with the predicted quantum corrections to the escape rate so that it was not possible to establish the accuracy of these predicted corrections to the thermal escape rate.¹⁹

In this Rapid Communication, we report measurements of MQT in a current-biased junction shunted by a thin-film resistor designed to be a good approximation to the resistively shunted junction (RSJ) model in the underdamped limit. The relevant parameters were measured in the classical regime. At the lowest temperature, the suppression of $\Gamma(T)$ by damping is in excellent agreement with predictions. Furthermore, the enhancement of $\Gamma(T)$ over the thermal activation rate for $T_{cr} < T < 3T_{cr}$ agrees well with the theory of Grabert and Weiss.¹⁰

In the RSJ model the current-biased Josephson junction is represented as a particle moving in a tilted washboard potential. The zero voltage state corresponds to the confinement of the particle in one of the wells, while the voltage state corresponds to the particle running down the washboard. For a bias current I less than the critical current I_0 the energy barrier separating the two states is²¹

$$\begin{aligned} \Delta U &= (I_0\Phi_0/\pi)[(1-s^2)^{1/2} - s \cos^{-1}s] \quad (s < 1) \\ &= (2\sqrt{2}I_0\Phi_0/3\pi)(1-s)^{3/2} \quad (s \ll 1), \end{aligned} \quad (1)$$

the frequency of small oscillations at the bottom of the well is $\omega_p = \omega_{p0}(1-s^2)^{1/4}$, and the damping is represented by the quality factor $Q = \omega_p RC$; where $s = I/I_0$, $\omega_{p0} = (2\pi I_0/C\Phi_0)^{1/2}$, and $\Phi_0 = h/2e$. The relevant junction parameters are thus I_0 , the self-capacitance C , and the shunt resistance R .

We report here the results of a series of detailed measurements on a single junction; data from a second junction were consistent with them. The junction was patterned photolithographically on an unoxidized Si chip (see inset, Fig. 1). The shunt resistor consisted of a 20-nm-thick Au (25 wt. % Cu) film in a 5 μm wide, L-shaped strip connected to a 1-mm² cooling fin. After sputtering and etching the 200-nm-thick Nb base electrode we deposited a 200-nm-thick insulating layer of SiO. The Nb film was oxidized and a 200 nm film of Pb (5 wt. % In) was deposited to give a nominal junction area of $5 \times 10 \mu\text{m}^2$. The counterelectrode provided a ground plane over the shunt resistor, reducing its inductance L_s to an estimated value of 3 pH; the estimated capacitance C_s between the shunt and the ground plane was less than 0.1 pF. Thus, for $\omega_p/2\pi \approx 10$ GHz the stray reactances $\omega_p L_s \approx 0.2 \Omega$ and $1/\omega_p C_s \approx 160 \Omega$ provided a negligible loading compared with the shunt resistance of about 10 Ω . The skin depth of the shunt at 10 GHz is estimated to be 1 μm , much greater than the thickness, so that the resistance was constant up to frequencies well beyond 10 GHz.

The junction was mounted at the end of the microwave filter used in earlier experiments.¹⁵ Using the same mount in a separate experiment over the temperature range 1.5 to 4.2 K, we used the classical phenomenon of resonant activation²² in the frequency range 7 to 12 GHz to measure the capacitance and resistance of the junction (including any contributions from the shunt and the leads). We found $C = 4.28 \pm 0.34$ pF, the uncertainty arising from variations with frequency due to standing-wave resonances in the leads. The resistance was $14 \pm 9 \Omega$, the error arising almost entirely from uncertainties in the theory for low Q junctions (see Ref. 22). We obtained a more accurate estimate of R from the current-voltage characteristic, which was linear with a value of $9.3 \pm 0.1 \Omega$ for voltages below the sum of the energy gaps in the superconductors. This shunt resistance was substantially less than both the quasiparticle resistance of the tunnel junction and the impedance presented to the junction by the mount.¹⁵

To make measurements in the quantum limit we attached the mount to the mixing chamber of a dilution refrigerator. The leads connected to the mount were extensively filtered.¹⁵ We determined the escape rate from the zero voltage state using a current ramp, obtaining current distributions of at least 10^4 events over a range of temperatures from 18 to 830 mK. The cooling fin on the shunt resistor reduced both the temperature attained by the shunt after the junction switched to the voltage state, and the time required for the shunt to cool down after the bias current was turned off. The time to cool to a refrigerator temperature of 18 mK was about 100 ms, and we allowed 300 ms to elapse between switching off the bias current and beginning the next current ramp. We measured temperatures from 18 to 35 mK using a ⁶⁰Co nuclear thermometer attached to the junction mount. From 60 to 850 mK we used a Ge resistance thermometer, calibrated in a separate experiment²³ against a noise thermometer involving a dc SQUID. From 35 to 60 mK we interpolated the temperature with a carbon resistance thermometer.

TABLE I. Temperature dependence of critical current: $I_0^{(0)}$ with no corrections, $I_0^{(c)}$ with classical corrections, and $I_0^{(c,q)}$ with classical and quantum corrections; σ is the standard deviation.

Temperature (mK)	$I_0^{(0)}$ (μA)	$I_0^{(c)}$ (μA)	$I_0^{(c,q)}$ (μA)	σ (μA)
830	24.895	24.880	24.882	0.012
627	24.900	24.887	24.890	0.010
453	24.882	24.871	24.875	0.007
333	24.877	24.867	24.872	0.006
267	24.870	24.861	24.867	0.004
202	24.876	24.868	24.876	0.003
158	24.868	24.861	24.871	0.002
126	24.869	24.862	24.874	0.002
104	24.867	24.861	24.875	0.002
93	24.864	24.858	24.873	0.002
82	24.859	24.853	24.870	0.002

We measured the critical current from the exponential dependence of $\Gamma(T)$ on I in the thermal activation regime in which $\Gamma(T) = a_i f_p \exp(-\Delta U/k_B T)$, where $f_p = \omega_p/2\pi$. If a_i were unity, we see from the expression for $\Gamma(T)$ and the cubic-well approximation for ΔU [Eq. (1)] that a plot of $[\ln \omega_p(I)/2\pi\Gamma(I)]^{2/3}$ vs I would be a straight line intersecting the current axis at I_0 . Table I shows the values of the intercepts $I_0^{(0)}$ obtained in this manner from data taken at 11 temperatures. Also shown are the values of the critical current $I_0^{(c)}$ after we made the classical corrections for the use of the cubic approximation for the barrier height and for the departure of a_i from unity,¹⁵ and the values $I_0^{(c,q)}$ after we applied the quantum corrections to the escape rate.¹⁰ The quoted random errors are the stan-

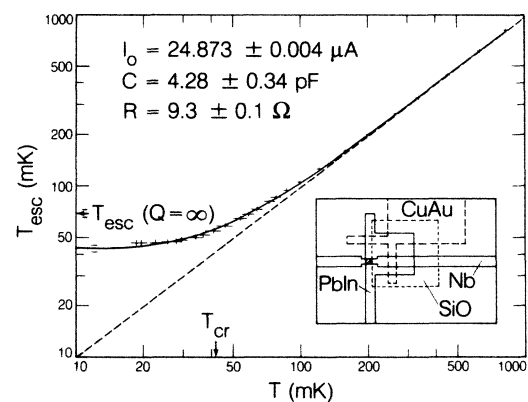


FIG. 1. T_{esc} vs T for a junction with the listed values of I_0 , C , and R . Vertical error bars indicate uncertainty in the junction parameters; horizontal error bars indicate systematic uncertainty in the temperature calibration. The solid curve is theory, with an uncertainty (arising largely from the error in C) indicated by two horizontal bars. T_{cr} for this junction and T_{esc} for an undamped junction are indicated with arrows; the indicated uncertainty in $T_{\text{esc}}(Q = \infty)$ arises predominantly from the uncertainty in I_0 . Dashed line is $T_{\text{esc}} = 0.985T$. Inset shows junction configuration.

TABLE II. Junction parameters, values of $T_{\text{esc}}^{\text{expt}}$ measured at 18 mK and extrapolated to 0 mK, and corresponding predicted values of $T_{\text{esc}}^{\text{p}}$.

I_0	C	R	I	$\omega_p/2\pi$	Q	T	$T_{\text{esc}}^{\text{expt}}$	$T_{\text{esc}}^{\text{p}}$
$24.873 \pm 0.004 \mu\text{A}$	$4.28 \pm 0.34 \text{ pF}$	$9.3 \pm 0.1 \Omega$	$24.710 \mu\text{A}$	$7.2 \pm 0.3 \text{ GHz}$	1.77 ± 0.07	$\left\{ \begin{array}{l} 18 \text{ mK} \\ 0 \text{ mK} \end{array} \right.$	$46 \pm 2 \text{ mK}$	$45 \pm 2 \text{ mK}$
							$45 \pm 2 \text{ mK}$	$43 \pm 2 \text{ mK}$

standard deviation obtained from a least-squares analysis. We observe that the critical current $I_0^{(c,q)}$ does not vary significantly over the temperature range from 830 to 82 mK, implying that our data are consistent with the predictions for quantum corrections. However, since we wish to *test* the applicability of the quantum corrections we have chosen to take as the temperature-independent critical current the average of the critical currents at the highest four temperatures where the quantum corrections are less than the random errors. In computing this average, we weighted the values of the critical currents according to their uncertainties.

The escape rates are presented in the form of the escape temperature T_{esc} defined by $\Gamma(T) = f_p \exp(-\Delta U/k_B T_{\text{esc}})$. In Fig. 1 we plot T_{esc} vs T , where we have calculated T_{esc} at the value of I at which the distribution of switching events is a maximum. Because ω_p and Q depend in I , their values change slightly with temperature. The solid line represents the theoretical predictions. Above the crossover temperature¹⁰ $T_{\text{cr}} = \hbar f_p [(1 + \alpha^2)^{1/2} - \alpha]/k_B$, where $\alpha = 1/2Q$, we have used Eq. (11) of Ref. 10. Below T_{cr} we computed $\Gamma(T)$ from Eqs. (7) and (9) and the tabulated values of f' in Ref. 8 using the numerical technique of Ref. 2. The dashed line represents the prediction¹¹ for thermal activation, $T_{\text{esc}} = 0.985T$; the factor 0.985 arises from the departure of a_i from unity.¹¹ We observe that experiment and theory are in good agreement over the entire temperature range. For $T > 200$ mK the measured

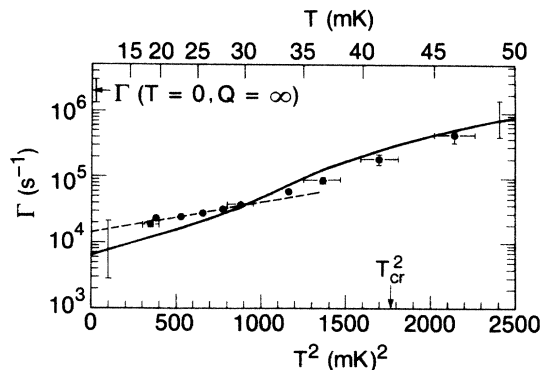


FIG. 2. Solid circles are $\Gamma(T)$ vs T^2 for $I = 24.71 \mu\text{A}$; vertical error bars represent statistical uncertainty. Solid curve is prediction of Ref. 10 with vertical error bars arising from systematic errors in I_0 , C , and R . Dashed line indicates a least-squares linear fit of the data below 30 mK to $\ln\Gamma(\text{s}^{-1}) = A + BT^2$; the asymptote for the data is $A = 9.4 \pm 0.5$, while theory predicts $A = 8.8 \pm 1.0$. The slope for the data is $B = (1.3 \pm 0.1)/\text{mK}^2$, while theory gives $B = (1.9 \pm 0.2)/\text{mK}^2$. Arrows indicate the predicted values of T_{cr}^2 and the escape rate at $T=0$ and $Q=\infty$.

values of T_{esc} are very nearly equal to T , whereas for $T_{\text{cr}} = 42 \pm 2 \text{ mK} < T < 3T_{\text{cr}}$ the measured values of T_{esc} lie significantly above the classical predictions. At the lowest temperature, 18 mK, the measured and predicted values of T_{esc} are in excellent agreement, and substantially lower than the value predicted for the undamped case (see Table II).

We also measured T_{esc} with I_0 reduced by a magnetic field to lower T_{cr} to 14 mK, and found that T_{esc} followed the classical prediction down to about 30 mK, flattening somewhat at lower temperatures. This experiment demonstrated that the flattening of T_{esc} was not due to extraneous noise sources.¹⁵

To investigate the low-temperature behavior of $\Gamma(T)$ in more detail, in Fig. 2 we plot $\ln\Gamma(T)$ vs T^2 for fixed-bias current. The data always lie within a factor of 2 of the predicted curve. The general behavior of the data and the predictions is rather similar: In each case $\ln\Gamma(T)$ scales as T^2 below about 30 mK, and increases somewhat more rapidly at higher temperatures. However, at low temperatures the measured slope is about 30% below the predicted value, for reasons that are not known. We note that if we vary the junction parameters used to obtain the predicted curve within the limits set by the experimental uncertainties, this curve is essentially displaced vertically, with an insignificant change in slope. We observe that the extrapolated value of $\Gamma(0)$ is within a factor of 2 of the predicted value which, in turn, has been reduced by a factor of about 300 from the value calculated in the absence of dissipation.

To test for the existence of quantum corrections to

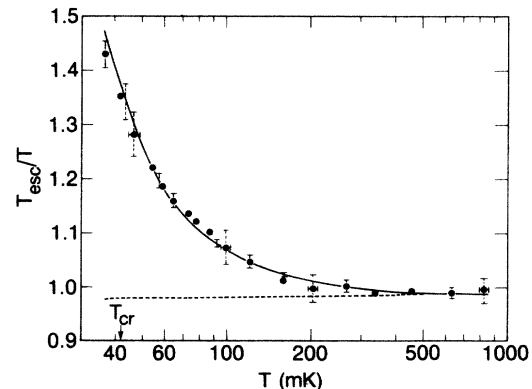


FIG. 3. T_{esc}/T vs T . Solid curve is prediction of Ref. 10; dashed line is the prediction of classical theory. $\Delta U/k_B T$ ranges from 12.4 to 14.0. Dashed error bars represent uncertainty in the temperature calibration, solid bars represent uncertainty in the junction parameters.

thermal activation for $T \geq T_{cr}$, in Fig. 3 we plot T_{esc}/T vs T . The solid line represents the theory of Grabert and Weiss.¹⁰ As T is lowered to T_{cr} we see that T_{esc}/T becomes greater than unity, indicating that the escape temperature exceeds the predictions for thermal activation: At T_{cr} , T_{esc} is about 40% above the thermal value. The good agreement between the data and the theory over the entire temperature range provides the first unambiguous verification of the Grabert-Weiss theory for the enhanced escape rate.

In summary, the measured escape rate of a current-biased resistively shunted Josephson tunnel junction from the zero voltage state is in good agreement with theoretical predictions over the temperature range from 18 to 830 mK. In particular, the values of Γ and T_{esc} measured at the lowest temperature and extrapolated to $T=0$ are in excellent agreement with predictions, providing quantitative evidence for the validity of the theory of MQT in the

presence of damping. Furthermore, for $T_{cr} < T < 3T_{cr}$ the measured values of T_{esc} lie significantly above the classical theory in good agreement with the predicted quantum corrections to the escape rate.

Two of us (A.N.C. and J.M.M.) thank the University of California at Berkeley, the National Science Foundation, and IBM for financial support during the course of this research. We would also like to thank H. Grabert and S. Linkwitz for help with the numerical predictions, J. E. Lukens and F. Wellstood for valuable conversations, and F. Wellstood for developing the noise thermometry. This work was supported by the Director, Office of Energy Research, Office of Basic Energy Sciences, Materials Sciences Division of the U.S. Department of Energy under Contract No. DE-AC03-76SF00098.

*Present address: Service de Physique du Solide et de Resonance Magnetique, Centre d'Etudes Nucleaires de Saclay, 91191 Gif-sur-Yvette Cédex, France.

¹A. O. Caldeira and A. J. Leggett, *Ann. Phys. (N.Y.)* **149**, 374 (1983); **153**, 445(E) (1984).

²L. D. Chang and S. Chakravarty, *Phys. Rev. B* **29**, 130 (1984); **30**, 1566(E) (1984).

³I. Affleck, *Phys. Rev. Lett.* **46**, 388 (1981).

⁴A. I. Larkin and Y. N. Ovchinnikov, *Pis'ma Zh. Eksp. Teor. Fiz.* **37**, 322 (1983) [*JETP Lett.* **37**, 382 (1983)].

⁵H. Grabert, U. Weiss, and P. Hanggi, *Phys. Rev. Lett.* **52**, 2193 (1984).

⁶P. S. Riseborough, P. Hanggi, and E. Friedkin, *Phys. Rev. A* **32**, 489 (1985).

⁷W. Zwerger, *Phys. Rev. A* **31**, 1745 (1985).

⁸H. Grabert, P. Olschowski, and U. Weiss, *Phys. Rev. B* **32**, 3348 (1985); **36**, 1931 (1987).

⁹A. I. Larkin and Y. N. Ovchinnikov, *Zh. Eksp. Teor. Fiz.* **85**, 1510 (1983); **86**, 719 (1984) [*Sov. Phys. JETP* **58**, 876 (1983); **59**, 420 (1984)].

¹⁰H. Grabert and U. Weiss, *Phys. Rev. Lett.* **53**, 1787 (1984).

¹¹H. A. Kramers, *Physica* **7**, 284 (1940).

¹²W. den Boer and R. de Bruyn Ouboter, *Physica B* **98**, 185 (1980); D. W. Bol, R. van Weelderen, and R. de Bruyn Ouboter, *ibid.* **122**, 2 (1983); D. W. Bol, J. J. F. Scheffer,

W. T. Giele, and R. de Bruyn Ouboter, *ibid.* **133**, 196 (1985).

¹³R. F. Voss and R. A. Webb, *Phys. Rev. Lett.* **47**, 265 (1981).

¹⁴L. D. Jackel, J. P. Gordon, E. L. Hu, R. E. Howard, L. A. Fetter, D. M. Tennant, R. W. Epworth, and J. Kurkujärvi, *Phys. Rev. Lett.* **47**, 697 (1981).

¹⁵J. M. Martinis, M. H. Devoret, and J. Clarke, *Phys. Rev. Lett.* **55**, 1908; *Phys. Rev. B* **35**, 4682 (1987). The latter reference includes a list of earlier experimental papers.

¹⁶S. Washburn, R. A. Webb, R. F. Voss, and S. M. Faris, *Phys. Rev. Lett.* **54**, 2712 (1985); S. Washburn and R. A. Webb, *Ann. N.Y. Acad. Sci.* **480**, 66 (1986).

¹⁷D. B. Schwartz, B. Sen, C. N. Archie, and J. E. Lukens, *Phys. Rev. Lett.* **55**, 1547 (1985).

¹⁸H. Grabert, P. Olschowski, and U. Weiss, *Phys. Rev. Lett.* **57**, 265 (1986); D. B. Schwartz, B. Sen, C. N. Archie, and J. E. Lukens, *ibid.* **57**, 266 (1986).

¹⁹J. E. Lukens (private communication).

²⁰A. D. Zaiken and S. V. Panyukov, *Pis'ma Zh. Eksp. Teor. Fiz.* **43**, 518 (1986) [*JETP Lett.* **43**, 670 (1986)].

²¹T. A. Fulton and L. N. Dunkleberger, *Phys. Rev. B* **9**, 4760 (1974).

²²M. H. Devoret, J. M. Martinis, D. Esteve, and J. Clarke, *Phys. Rev. Lett.* **53**, 1260 (1984).

²³F. Wellstood (unpublished).